



IUTAM Symposium Analytical Methods in Nonlinear Dynamics

Analytical control of homoclinic bifurcation of the hilltop saddle in a noncontact atomic force microcantilever

Valeria Settimi^a, Giuseppe Rega^{a,*}, Stefano Lenci^b

^aDepartment of Structural and Geotechnical Engineering, Sapienza University of Rome, Via A. Gramsci 53, 00197 Rome, Italy

^bDepartment of Civil and Building Engineering, and Architecture, Polytechnic University of Marche, Via Breccie Bianche, 60131 Ancona, Italy

Abstract

A control procedure of global dynamics is applied to a reduced order model of noncontact AFM with the aim to shift the homoclinic bifurcation involving the system hilltop saddle. The method consists of adding to the system harmonic excitation controlling superharmonics to be properly identified by solving an optimization problem. The analytical bifurcation threshold is determined through the asymptotic Melnikov method, for the reference system and for the controlled system. The practical effect of the control as regards possibly increasing the system overall robustness by shifting the start of the erosion of the safe basin is then numerically investigated by means of a dynamical integrity analysis based on the evolution of basins of attraction.

© 2016 The Authors. Published by Elsevier B.V. This is an open access article under the CC BY-NC-ND license

(<http://creativecommons.org/licenses/by-nc-nd/4.0/>).

Peer-review under responsibility of organizing committee of IUTAM Symposium Analytical Methods in Nonlinear Dynamics

Keywords: Noncontact AFM; Global control; Melnikov Method; Hilltop saddle; Homoclinic bifurcation; Basin erosion.

1. Introduction

In Atomic Force Microscope (AFM) literature several control techniques have been proposed in the last decades to improve microscope performances or avoid unwanted behaviors^{1,2,3}. They are mostly based on feedback methods aimed at stabilizing single suitable responses, so their effects on the overall dynamics are generally unknown. In particular, recent studies have shown that, while being generally effective in realizing the specific aim for which it is designed⁴, the insertion of an external feedback control in a noncontact AFM model causes a generalized reduction of the stability region and a dangerous decrease of system safety with respect to the unwanted jump to contact phenomenon⁵.

Yet, from a practical stability perspective, an acceptable system-dependent residual integrity is needed to guarantee secure AFM operation since it is nowadays well known that the safety of a nonlinear system depends not only on stability of its solutions but also on the uncorrupted basins of attraction surrounding them⁶. Thus, focusing on the preservation of dynamical integrity, it is worth exploiting whether a non-feedback control technique specifically aimed at favorably affecting a global bifurcation event which triggers basins erosion can also work for the AFM system and reduce the basin erosion which leads to the loss of safety. The method⁷ consists of optimally modifying the shape

*Corresponding author. Tel.: +39-06-49919195 ; fax: +39-06-49919192.

E-mail address: giuseppe.rega@uniroma1.it

of the reference harmonic excitation to shift the occurrence of the global event (i.e., homo/heteroclinic bifurcation of some saddle) which triggers the sudden fall down of the dynamical integrity profiles, thus obtaining an overall control of the dynamics and an enlargement of the system safe region in parameters space. Usually, global bifurcations triggering erosion involve the stable and unstable manifolds of the hilltop saddle; in this case, their occurrence can be analytically detected by the asymptotic Melnikov method⁸, and their control has proved to be effective in somehow delaying the erosion also when the actual fall down of the profiles is likely due to other secondary bifurcations which involve internal saddles⁹.

In the light of this, the present work is focused on the application of the control method to the main bifurcation event involving the hilltop saddle; the analytical procedure aimed at detecting the critical value of excitation amplitude corresponding to the manifolds intersection is applied to the general system with N superharmonics (included the reference harmonic case). The theoretical results are then numerically verified for the case of one controlling superharmonic, and for different values of the forcing frequency around the fundamental resonance, which has resulted to be a very critical region for the system^{4,10}. Finally, the evolution of the basins of attraction for the controlled system is investigated with the aim to point out the effect of the bifurcation shift on the evolution of the basins erosion.

2. Control of homoclinic bifurcation of hilltop saddle

2.1. AFM model

The control procedure is applied to a reduced model of noncontact AFM already studied in¹⁰ (see figure 1(a)), whose equation of motion in the case of horizontal and harmonic scan excitation is:

$$\ddot{x} + \alpha_1 \dot{x} + \alpha_3 x^3 + \frac{\Gamma_1}{(1+x)^2} = -\rho_1 \dot{x} - x\mu_1 \omega_u^2 U_1 \sin(\omega_u t) \quad (1)$$

where x is the transverse microcantilever displacement; α_1 , α_3 are linear and cubic stiffness terms; ρ_1 is the linear damping coefficient; Γ_1 is the attractive Lennard-Jones like atomic interaction coefficient¹¹; U_1 is the amplitude of the horizontal parametric-like excitation and ω_u is the relevant forcing frequency.

The operation domain of the noncontact AFM must be such to avoid the jump to contact with the scanned sample. In dynamical system terms, this is ascertained by considering the undamped, unforced version of (1)

$$\ddot{x} + \alpha_1 \dot{x} + \alpha_3 x^3 + \frac{\Gamma_1}{(1+x)^2} = 0 \quad (2)$$

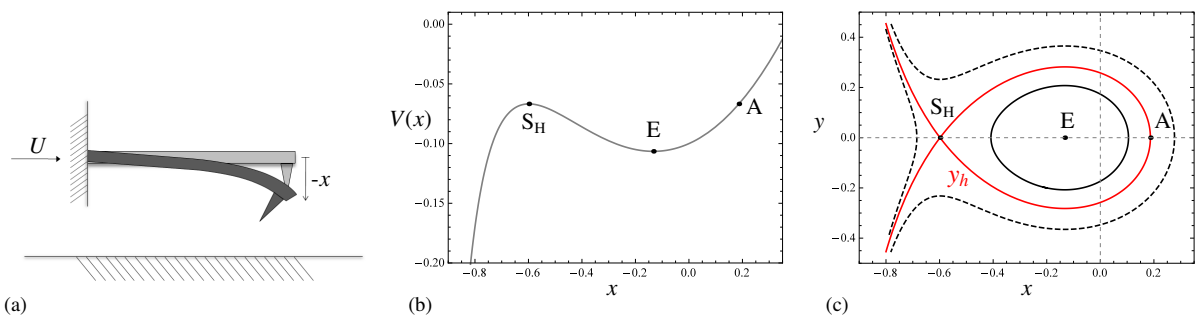


Fig. 1: AFM microcantilever (a), potential $V(x)$ (b), and unperturbed phase space (c) for $\alpha_1 = 1, \alpha_3 = 0.1, \Gamma_1 = 0.1$. In (c), homoclinic orbit y_h (solid red), periodic orbit (solid black), unbounded orbit (dashed black), equilibrium point (E), hilltop saddle point (S_H) are reported.

whose Hamiltonian reads

$$\begin{cases} \dot{x} = \frac{\partial H}{\partial y} \\ \dot{y} = -\frac{\partial H}{\partial x} \end{cases} \quad H(x, y) = +\frac{y^2}{2} + V(x) = +\frac{y^2}{2} + \frac{\alpha_1 x^2}{2} + \frac{\alpha_3 x^4}{4} - \frac{\Gamma_1}{1+x} \quad (3)$$

with the associated single potential well with left (i.e., towards the sample position $x = -1$) contact direction (escape), as shown in figure 1(b). The unperturbed state space is depicted in figure 1(c), where the two fixed points of the time-independent problem, the stable equilibrium (E) of the cantilever tip under elastic (α_1, α_3) and atomic interaction (Γ_1) forces and the corresponding hilltop saddle (S_H), are reported for a given set of values of the governing parameters.

The homoclinic orbit of the saddle is represented by the red curve in figure 1(c), and separates the inner region of bounded periodic solutions, representing the safe domain for noncontact AFM operation, from the outer region of unbounded solutions leading to the unwanted jump to contact phenomenon. Its expression, obtained from the Hamiltonian system (3), reads

$$y_h(x) = \frac{dx_h}{dt} = \pm \sqrt{2(V(x_{S_H}) - V(x))} \quad (4)$$

where x_{S_H} is the coordinate of the hilltop saddle. The integral (4) cannot be obtained in closed form but has to be computed numerically. It is worth reminding that such a curve represents the right unstable ($W^u(S_H)$) and stable ($W^s(S_H)$) manifolds of the hilltop saddle, which coincide with each other due to the unperturbed nature of the Hamiltonian system (see sketch in figure 2).

2.2. Analytical procedure

The control procedure aims at shifting the bifurcation threshold by optimally modifying the excitation shape⁷, i.e. by adding controlling superharmonics to the harmonic excitation of the system (1):

$$\ddot{x} + \alpha_1 x + \alpha_3 x^3 + \frac{\Gamma_1}{(1+x)^2} = -\rho_1 \dot{x} - x\mu_1 \omega_u^2 U_1 \sum_{j=1}^N \frac{U_j}{U_1} \sin(j\omega_u t + \Psi_j) \quad (5)$$

where U_1 is the horizontal parametric-like reference excitation while U_j and Ψ_j are the amplitudes and phases of the controlling superharmonics.

The presence of damping and excitation in system (5) causes the separation of the stable and unstable manifolds of the Hamiltonian system (1) (see figure 2), which may remain disjoint or intersect depending on the value of the excitation parameters. The critical situation of manifolds tangency corresponds to the occurrence of a global homo-

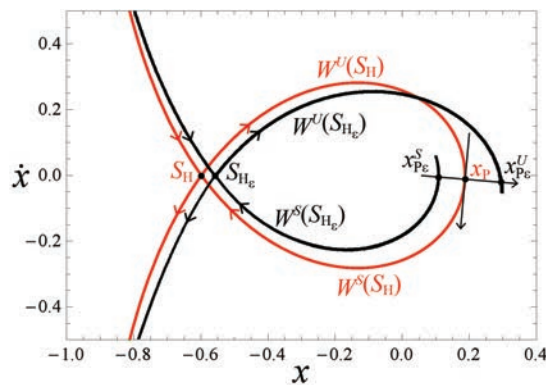


Fig. 2: Qualitative behavior of the stable (W^s) and unstable (W^u) manifolds of the hilltop saddle for the Hamiltonian system (red) and the ε -perturbed, forced, damped system (black).

clinic bifurcation, which can be analytically detected by the classical Melnikov method. Following the method, and in presence of weak excitation and damping, the system (5) can be expressed as an ε -perturbation of the Hamiltonian system (3):

$$\begin{cases} \dot{x} = y \\ \dot{y} = -\alpha_1 x - \alpha_3 x^3 - \frac{\Gamma_1}{(1+x)^2} + \varepsilon(-\rho_1 y - x\mu_1 \omega_u^2 U_1 \sum_{j=1}^N \frac{U_j}{U_1} \sin(j\omega_u t + \Psi_j)) \end{cases} \quad (6)$$

where ε is a smallness parameter. To the first order of the underlying asymptotic expansion, the distance between the stable ($W^s(S_{H\varepsilon})$) and unstable ($W^u(S_{H\varepsilon})$) manifolds of the perturbed system is furnished by the Melnikov integral:

$$\begin{aligned} \mathcal{M}(t_0) &= \int_{-\infty}^{+\infty} y_h(t) (-\rho_1 y_h(t) - x_h(t) \mu_1 \omega_u^2 U_1 \sum_{j=1}^N \frac{U_j}{U_1} \sin(j\omega_u(t + t_0) + \Psi_j)) dt \\ &= 2\rho_1 I_1 - 2\mu_1 \omega_u^2 U_1 I_2(\omega_u) h(m) \end{aligned} \quad (7)$$

where

$$I_1 = - \int_{x_A}^{x_{S_H}} y_h(x) dx, \quad I_2(j\omega_u) = \int_{x_A}^{x_{S_H}} x \sin(j\omega_u \int_{x_A}^x \frac{dr}{y_h(r)}) dx$$

are integrals to be numerically computed, and

$$h(m) = \sum_{j=1}^N h_j \cos(j\omega_u t_0 + \Psi_j), \quad h_j = \frac{U_j I_2(j\omega_u)}{U_1 I_2(\omega_u)}$$

is 2π -periodic with zero mean value ($m = \omega_u t_0$).

The tangency of the stable and unstable manifolds, i.e. the occurrence of the homoclinic bifurcation, corresponds to a simple zero of the Melnikov integral $\mathcal{M}(t_0) = 0$ for some t_0 :

$$U_{1,cr} = \frac{\rho_1 I_1}{\mu_1 \omega_u^2 |I_2(\omega_u)| M}, \quad \text{with} \quad \begin{cases} M = M^+ = \max_{m \in [0, 2\pi]} \{h(m)\}, & I_2(\omega_u) > 0 \\ M = M^- = -\min_{m \in [0, 2\pi]} \{h(m)\}, & I_2(\omega_u) < 0 \end{cases} \quad (8)$$

Note that in presence of the sole reference harmonic excitation ($j = 1$) $h_1 = 1$ and $M = 1$.

The aim of the control method is to shift the occurrence of the homoclinic tangency to the highest possible value of the forcing amplitude, which corresponds to the following optimization problem⁷:

$$\begin{aligned} &\text{Maximize} \quad \min_{m \in [0, 2\pi]} \{h(m)\}, \quad I_2(\omega_u) < 0 \\ &\text{Minimize} \quad \max_{m \in [0, 2\pi]} \{h(m)\}, \quad I_2(\omega_u) > 0 \end{aligned} \quad (9)$$

The optimization can be achieved by properly choosing h_j and Ψ_j , where $j = 1, 2, 3, \dots, N$ is the number of superharmonics to be added to the system. To measure the improvement obtainable with respect to the reference harmonic excitation, the gain G is introduced: $G = U_{1,cr}/U_{1,cr}^h = 1/M$, where $U_{1,cr}^h$ represents the critical amplitude for the reference harmonic system. Setting $\Psi_j = 0$ and focusing on the addition on one superharmonic, i.e. $j = 2$, the evolution of $h(m)$ for varying h_2 is reported in figure 3(a). Here, the black curve corresponds to the presence of the sole harmonic excitation ($h_2 = 0$) with the minimum of the curve which is equal to -1 ($G = 1$), the orange curve is obtained for $h_2 = 0.353553$ and is the solution of the optimization problem (9), as its minimum reaches the maximum value in $h(m) = -0.707107$, corresponding to the maximal theoretical gain $G = 1.4142$ ⁷. Finally, the grey curve, obtained for $h_2 = 0.8535$, shows the minimum equal to -1 , as in the harmonic case. Referring to such three cases, the relevant homoclinic bifurcation thresholds detected by means of the Melnikov method are reported in figure 3(b) in the excitation parameters plane (ω_u, U_1). The outcomes confirm that the presence of the optimal superharmonic into the model (orange curve in figure) manages to shift the bifurcation threshold to higher values of the forcing amplitude with respect to the harmonic case (black curve), apart from the region around the "anti-resonant" frequency $\omega_u \approx 1.03$ at which the threshold goes to infinity due to the first order nature of the Melnikov approximation. It is worth noting

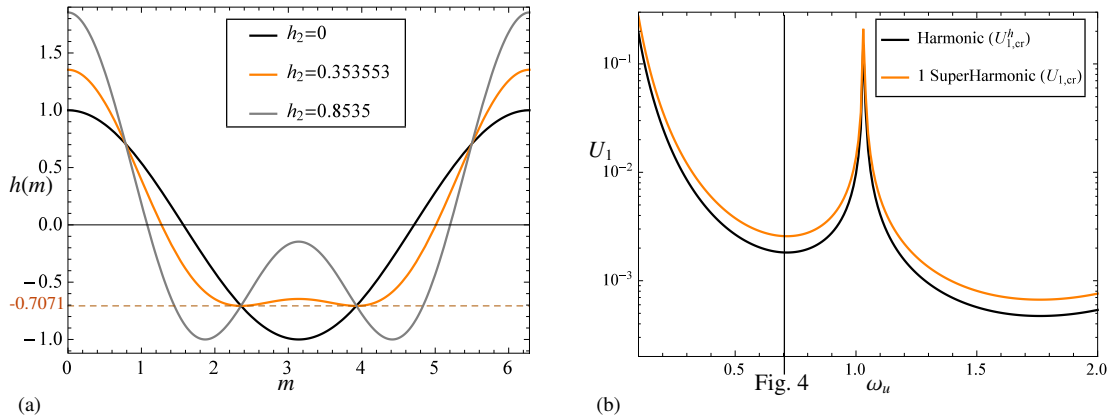


Fig. 3: $h(m)$ for different values of the h_2 parameter (a) and relevant analytical bifurcation thresholds in the $\omega_u - U_1$ plane (b). Black curve: reference harmonic system; Orange curve: system with superharmonic $h_2 = 0.353553$ (optimal); Grey curve: system with superharmonic $h_2 = 0.8535$.

that the black curve represents also the results obtained for the case $h_2 = 0.8535$ (grey curve in figure 3(a)), meaning that in this case the presence of the superharmonic is non influential in the occurrence of the global bifurcation.

2.3. Numerical validation

The analytical results have been validated by the numerical detection of the hilltop manifolds for different values of forcing amplitude and for a frequency range which includes values to the right and left of the fundamental resonance $\omega_1 = 0.8357$. Figure 4 shows the tangency between the stable (red) and unstable (blue) hilltop manifolds at $\omega_u = 0.7$ for the system with harmonic excitation (figure 4(a)) at $U_1 = U_{1,cr}^h = 0.001823$ and with optimal superharmonic ($U_2/U_1 = -0.53898$, figure 4(b)) at $U_1 = U_{1,cr} = 0.002578$ (which corresponds to $G = 1.4142$). Beyond confirming the accuracy of the results furnished by the analytical Melnikov procedure, the outcomes highlight a qualitatively different trend of the hilltop manifolds in the two cases, with the tangent point being shifted along the stable manifold by the addition of the optimal superharmonic. It is worth noting that the increase of the bifurcation threshold occurs for negative values of the amplitude of the controlling superharmonic, while positive amplitudes produce a worsening effect of the global dynamical behavior. From an operational point of view, the same result can be achieved by applying positive superharmonics with a phase shift $\Psi_2 = \pi$.

The effect of different superharmonics can be observed in figure 5, obtained at $\omega_u = 0.7$ and $U_1 = U_{1,cr}^h = 0.001823$ for the system with the optimal superharmonic $U_2/U_1 = -0.53898$ (figure 5(a)) and with the superharmonic $U_2/U_1 =$

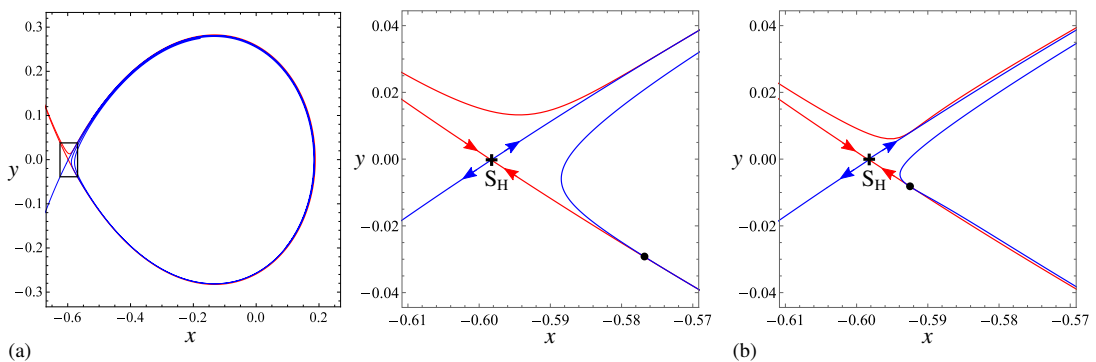


Fig. 4: Stable (red) and unstable (blue) manifolds of the hilltop saddle S_H , and enlargement, for the reference harmonic system at $U_{1,cr}^h = 0.001823$ (a) and for the system with optimal superharmonic at $U_{1,cr} = 0.002578$ (b). Circle points identify one of the manifolds tangency points.

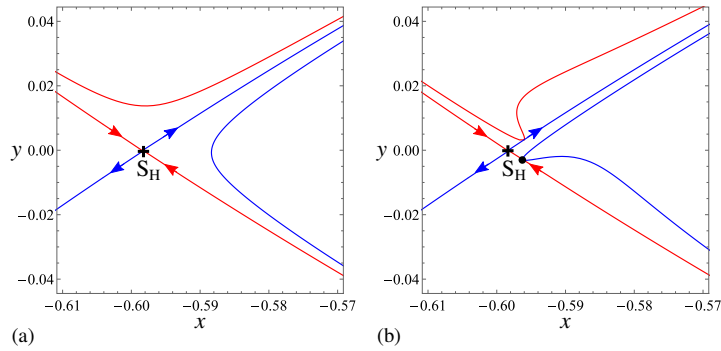


Fig. 5: Stable (red) and unstable (blue) manifolds of the hilltop saddle S_H for the system with optimal superharmonic (a) and for the system with superharmonic $h_2 = 0.8535$ (b) at $U_{1,cr}^h = 0.001823$. Circle points identify one of the manifolds tangency points.

-1.301 (corresponding to $h_2 = 0.8535$, figure 5(b)). The presence of the optimal controlling superharmonic causes the maximal separation of the hilltop manifolds, and the maximum gain G . Instead, for $U_2/U_1 = -1.301$, the manifolds intersect again, even if their pattern is rather different and the bifurcation point is shifted.

3. Effects of the control on the system dynamical robustness

In the previous section, the addition of controlling superharmonics into the model has shown to be a simple and efficient procedure for delaying the occurrence of the homoclinic bifurcation involving the manifolds of the hilltop saddle. The effects of such control on the evolution of the safe basin erosion are now discussed, by carrying out the analysis of the system dynamical integrity. In this respect, the safe basin is defined as the union of the classical basins of attraction inside the potential well, and the integrity measures used to quantify the erosion are the Global Integrity Measure (GIM), corresponding to the area of the safe basin, and the Integrity Factor (IF), which represents the radius of the largest circle inscribed into the safe basin and is a measure of its compact part¹². By numerically obtaining the basins of attraction for increasing values of the forcing amplitude, and by quantifying the basins integrity, the erosion profiles of figure 6 are obtained, for the system with harmonic excitation (black curves) and for the one with optimal superharmonic (orange curves), at frequency values before and after the fundamental resonance $\omega_1 = 0.8357$.

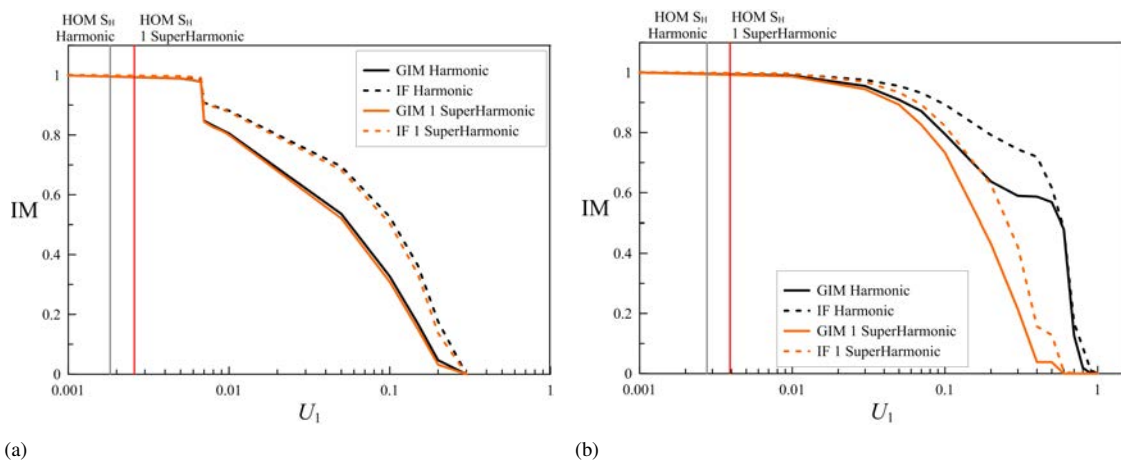


Fig. 6: Erosion profiles as a function of the forcing amplitude U_1 for the reference harmonic system (black) and for the system with optimal superharmonic (orange), at $\omega_u = 0.7$ (a) and at $\omega_u = 0.9$ (b). Dashed lines: profiles obtained with Integrity Factor (IF); Continuous lines: profiles obtained with Global Integrity Measure (GIM); IM: Integrity Measures.

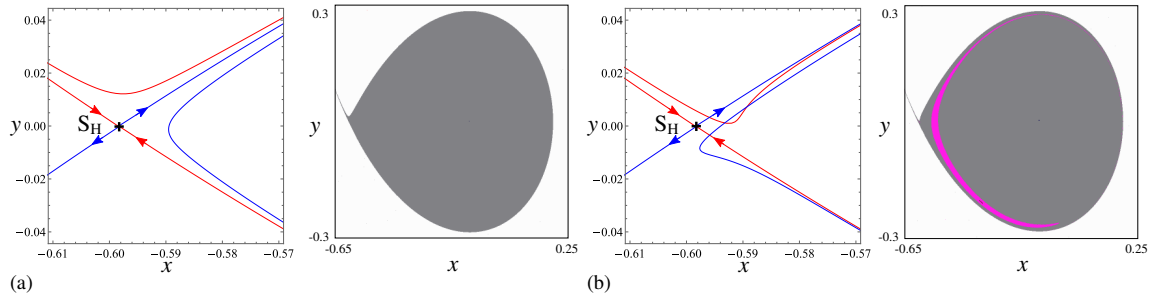


Fig. 7: Manifolds and basins of attraction for the system with optimal superharmonic at $U_1 = 0.002$ (a) and at $U_1 = 0.003$ (b), for $\omega_u = 0.7$.

The results highlight that the controlling superharmonic is not able to improve the system integrity, i.e to shift the profiles fall down to higher values of the forcing amplitude, different from what observed in several other systems with escape¹². Moreover, right of the fundamental resonance the controlled profiles result to be sharper than the harmonic ones, especially in their final part (see figure 6(b)), meaning that for high values of the forcing amplitude the control worsens the system robustness (this is anyway a well known behavior, detected in other literature systems¹²). To investigate the causes of this behavior, the evolution of the basins of attraction for increasing U_1 has been numerically investigated, for the reference harmonic system and for the system with optimal superharmonic, even if in this paper only the results related to the latter are reported for the sake of brevity. Figure 7 shows the behavior of the basins and manifolds before and after the homoclinic bifurcation at $U_1 = 0.002578$ for the controlled system at the left of the resonance ($\omega_u = 0.7$). Once the manifolds intersect, the unbounded solution basin which surrounds the potential well (white basin in figure) starts penetrating inside the well through fractal tongues from the outer edge. However, the safe basin erosion develops so slowly that it can be observed only through enlargements (not reported) of the basin border, and does not affect the basin size and, consequently, the slope of the erosion profiles. It is worth pointing out that just before the homoclinic bifurcation, at $U_1 = 0.00244$, inside the basin of the nonresonant 1-period solution (grey basin in figures 7 and 8) a new basin arises (pink basin in figures 7 and 8), corresponding to the competing resonant 1-period solution, and it grows to the detriment of the former as the amplitude increases (see¹⁰ for the detailed behavior of the reference system basins). In this situation, the safe basin is considered as the sum of the two basins of attraction, under the condition of total absence of the unbounded basin between them.

When the amplitude approaches the value $U_1 = 0.0067$ (numerically detected) corresponding to the profiles fall down, the two 1-period basins separate due to the penetration of the unbounded basin tongue, as reported in figure 8(b). As a consequence, the safe basin size is suddenly reduced and becomes coincident with the sole grey (nonresonant) basin (which is the bigger one), thus causing the sharp decrease of the profiles in figure 6(a), which actually occurred also in the absence of control. At this amplitude, the positive effects of the homoclinic bifurcation shift, occurred at considerably lower values of excitation amplitude, have been exhausted; in fact, the stable and unstable manifolds of

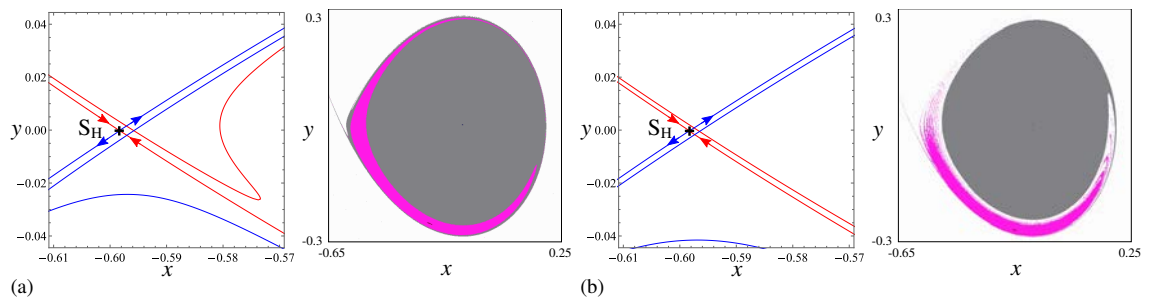


Fig. 8: Manifolds and basins of attraction for the system with optimal superharmonic at $U_1 = 0.005$ (a) and at $U_1 = 0.01$ (b), for $\omega_u = 0.7$.

the hilltop saddle clearly intersect each other. However, the presence of two basins inside the potential well suggests the presence of other internal saddles whose manifolds are responsible for the basins behavior inside the well.

After the fundamental resonance (see figure 6(b)), there is no more coexistence of the two competing resonant/nonresonant solutions¹⁰ and the safe basin corresponds to the main 1-period solution (apart from multiple period solutions occurring in very narrow ranges of the forcing amplitude). At these frequencies, the safe basin erosion develops slowly over a wide range of excitation amplitudes, and only for high relevant values, far away from the homoclinic bifurcation amplitude, the presence of secondary solutions causes the fall down of the erosion profile.

4. Conclusions

A control procedure aimed at shifting the occurrence of the homoclinic bifurcation involving the manifolds of the hilltop saddle has been applied to a reduced model of noncontact AFM, with also the practical objective to possibly increase the system robustness by shifting the start of the erosion phenomenon which leads to the undesired jump to contact to higher values of the forcing amplitude. The method, based on the introduction of controlling superharmonics into the model, has been analytically developed by applying the asymptotic first order Melnikov procedure to determine the occurrence of the homoclinic bifurcation. After that, the optimal superharmonic has been detected based on the universal optimization problem formulated in other literature works for various mechanical systems.

The results have been numerically validated and they have confirmed the efficiency of the control method in moving the global bifurcation to higher amplitude values, thus enhancing the system safe, i.e. non fractal, region mostly for frequencies around the fundamental resonance which are proved to be the most critical ones for the system^{4,10}.

However, different from other literature cases, the analysis of the basins evolution has shown that the control of the hilltop saddle manifolds does not manage to improve the system overall robustness with respect to the increasing forcing amplitude. This is likely due to the homoclinic bifurcation of the hilltop saddle being too far from the start of the safe basin erosion, and by the meaningful role played in this respect by other saddles present in the system. Preliminary investigations have pointed out the importance of the internal saddle on the boundary between the main in-well competing solutions, whose manifolds undergo two subsequent global bifurcations for forcing amplitudes very close to the start of the robustness reduction (i.e. to the erosion profile fall down), thus probably being responsible for the erosion development. Ongoing studies are addressed to the careful detection and control of these other global bifurcations, for which however the analytical Melnikov procedure cannot be applied and a fully numerical technique has to be implemented.

References

1. K. Yamasue, K. Kobayashi, H. Yamada, K. Matsushige, and T. Hikihara. Controlling chaos in dynamic-mode atomic force microscope. *Phys. Lett. A*, 373(35):3140–3144, 2009.
2. K. Yagasaki. Nonlinear dynamics and bifurcations in external feedback control of microcantilevers in atomic force microscopy. *Commun. Nonlinear Sci. Numer. Simul.*, 18(10):2926–2943, 2013.
3. I. Kirrou and M. Belhaq. Control of bistability in non-contact mode atomic force microscopy using modulated time delay. *Nonlinear Dyn.*, 81(1-2):607–619, 2015.
4. V. Settimi, O. Gottlieb, and G. Rega. Asymptotic analysis of a noncontact afm microcantilever sensor with external feedback control. *Nonlinear Dyn.*, 79(4):2675–2698, 2015.
5. V. Settimi and G. Rega. Influence of a locally-tailored external feedback control on the overall dynamics of a non-contact AFM model. *Int. J. Non-Linear Mech.*, 2015. doi: <http://dx.doi.org/10.1016/j.ijnonlinmec.2015.05.010>.
6. S. Lenci and G. Rega. Load carrying capacity of systems within a global safety perspective. Part II. Attractor/basin integrity under dynamic excitations. *Int. J. Non-Linear Mech.*, 46:1240–1251, 2011.
7. S. Lenci and G. Rega. A unified control framework of the nonregular dynamics of mechanical oscillators. *J. Sound Vib.*, 278:1051–1080, 2004.
8. S. Wiggins. *Global bifurcation and chaos: Analytical Methods*. Springer, 1988.
9. S. Lenci and G. Rega. Control of pull-in dynamics in a nonlinear thermoelastic electrically actuated microbeam. *J. Micromech. Microeng.*, 16:390–401, 2006.
10. G. Rega and V. Settimi. Bifurcation, response scenarios and dynamic integrity in a single-mode model of noncontact atomic force microscopy. *Nonlinear Dyn.*, 73:101–123, 2013.
11. S. Hornstein and O. Gottlieb. Nonlinear dynamics, stability and control of the scan process in noncontacting atomic force microscopy. *Nonlinear Dyn.*, 54:93–122, 2008.
12. G. Rega and S. Lenci. Dynamical integrity and control of nonlinear mechanical oscillators. *J. Vib. Control*, 14:159–179, 2008.